THE JOURNAL OF BIOLOGICAL CHEMISTRY Vol. 280, No. 20, Issue of May 20, pp. 19888–19894, 2005
Printed in U.S.A.

Receptor-regulated Dynamic *S*-Nitrosylation of Endothelial Nitric-oxide Synthase in Vascular Endothelial Cells*

Received for publication, November 18, 2004, and in revised form, March 10, 2005
Published, JBC Papers in Press, March 17, 2005, DOI 10.1074/jbc.M413058200

Phillip A. Erwin‡§, Alison J. Lin¶, David E. Golan¶‖, and Thomas Michel‡‡‡**

*From the ‡Cardiovascular and ‖Hematology Divisions, Brigham and Women's Hospital, ¶Department of Biological Chemistry and Molecular Pharmacology, Harvard Medical School, Boston, Massachusetts 02115, and **Veterans Affairs Boston Healthcare System, West Roxbury, Massachusetts 02132*

The endothelial isoform of nitric-oxide synthase (eNOS) is regulated by a complex pattern of post-translational modifications. In these studies, we show that eNOS is dynamically regulated by *S*-nitrosylation, the covalent adduction of nitric oxide (NO)-derived nitrosyl groups to the cysteine thiols of proteins. We report that eNOS is tonically *S*-nitrosylated in resting bovine aortic endothelial cells and that the enzyme undergoes rapid transient denitrosylation after addition of the eNOS agonist, vascular endothelial growth factor. eNOS is thereafter progressively renitrosylated to basal levels. The receptor-mediated decrease in eNOS *S*-nitrosylation is inversely related to enzyme phosphorylation at Ser^{1179}, a site associated with eNOS activation. We also document that targeting of eNOS to the cell membrane is required for eNOS *S*-nitrosylation. Acylation-deficient mutant eNOS, which is targeted to the cytosol, does not undergo *S*-nitrosylation. Using purified eNOS, we show that eNOS *S*-nitrosylation by exogenous NO donors inhibits enzyme activity and that eNOS inhibition is reversed by denitrosylation. We determine that the cysteines of the zinc-tetrathiolate that comprise the eNOS dimer interface are the targets of *S*-nitrosylation. Mutation of the zinc-tetrathiolate cysteines eliminates eNOS *S*-nitrosylation but does not eliminate NO synthase activity, arguing strongly that disruption of the zinc-tetrathiolate does not necessarily lead to eNOS monomerization *in vivo*. Taken together, these studies suggest that eNOS *S*-nitrosylation may represent an important mechanism for regulation of NO signaling pathways in the vascular wall.

Nitric oxide (NO)[1] is a reactive free radical gas that plays a central role in diverse signaling pathways (reviewed in Ref. 1). In mammals, NO is synthesized by three synthases responsible for (patho)physiologic NO signaling in the immune, neurological, and cardiovascular systems (reviewed in Ref. 2). Vascular endothelial cells robustly express the endothelial isoform of NO synthase (eNOS), a constitutive 135-kDa protein that is central to homeostatic mechanisms such as vasorelaxation, regulation of myocardial contractility, and blood platelet aggregation (reviewed in Ref. 3). Similar to all NO synthase (NOS) isoforms, eNOS functions as an obligate homodimer through an association mediated by a cysteine-complexed Zn^{2+} (zinc-tetrathiolate) at the dimer interface (4–6). eNOS activity is regulated by several dynamic phosphorylations and protein-protein interactions (reviewed in Ref. 7) that can be modulated following the activation of cell surface receptors by agonists such as the vascular endothelial growth factor (VEGF) (8).

In its canonical signaling role, NO acts as an intracellular messenger that increases cGMP concentration in target cells by activating guanylate cyclases (9). However, NO is also believed to signal through a guanylate cyclase-independent mechanism mediated by the interaction of reactive nitrogen oxides with the reduced cysteines of proteins, forming cysteine *S*-nitrosothiols that can effect changes in protein function (10). This process has been termed "*S*-nitrosylation" and appears to be a physiologically significant post-translational modification with functional consequences for signal protein activity (reviewed in Ref. 11). Dynamic receptor-modulated *S*-nitrosylation of a signal protein has not been reported previously, and the role of reversible *S*-nitrosylation in cellular signal transduction remains incompletely understood (11).

In this paper, we report that eNOS is tonically *S*-nitrosylated in bovine aortic endothelial cells (BAEC) and that the enzyme undergoes rapid transient denitrosylation after the addition of the eNOS agonist, VEGF or insulin. eNOS is thereafter progressively renitrosylated on a time course parallel to that of its return to resting activity levels after receptor-mediated activation. These studies also provide evidence that eNOS *S*-nitrosylation reversibly attenuates enzyme activity and identify a potentially important pathway for eNOS regulation.

EXPERIMENTAL PROCEDURES

Materials—Fetal bovine serum was from Hyclone (Logan, UT). All of the other cell culture reagents were from Invitrogen. VEGF, diethylamine-NONOate (DEA/NO), and wortmannin were from Calbiochem. Anti-eNOS monoclonal antibody was from Transduction Laboratories (Lexington, KY), and anti-phospho-$eNOS^{Ser\text{-}1179}$ antibody (phospho-Ser^{1177} in the human eNOS sequence) was from Cell Signaling Technologies (Beverly, MA). Polyclonal antibodies against eNOS phospho-Ser^{116}, eNOS phospho-Thr^{497} (phospho-Thr^{495} in the human sequence), and the HA epitope were from Upstate Biotechnology (Lake Placid, NY). Polyclonal eNOS anti-serum raised in rabbits in this laboratory was described previously (12). Monoclonal antibody 12CA5 used for immunoprecipitation of HA epitope-tagged eNOS was from Roche Applied Science. Anti-HA monoclonal antibody for immunoblot, and protein-A/G-agarose was from Santa Cruz Biotechnology (Santa Cruz, CA).

* This work was supported by National Institutes of Health Grants HL46457 and GM36259 (to T. M.) and HL32854 and HL070819 (to D. E. G.). The costs of publication of this article were defrayed in part by the payment of page charges. This article must therefore be hereby marked "*advertisement*" in accordance with 18 U.S.C. Section 1734 solely to indicate this fact.

§ Supported by a Howard Hughes Medical Institute predoctoral fellowship.

‡‡ To whom correspondence should be addressed: Cardiovascular Division, Brigham and Women's Hospital, Thorn Bldg. 1210A, 75 Francis St., Boston, MA 02115. Tel.: 617-732-7376; Fax: 617-732-5132; E-mail: tmichel@research.bwh.harvard.edu.

[1] The abbreviations used are: NO, nitric oxide; BAEC, bovine aortic endothelial cells; DEA/NO, diethylamine-NONOate; NOS, nitric-oxide synthase; eNOS, endothelial nitric-oxide synthase; HRP, horseradish peroxidase; L-NMA, *N*-methyl-L-arginine; HA, hemagglutinin; NOS, NO synthase; EGFP, enhanced green fluorescent protein; VEGF, vascular endothelial growth factor; ANOVA, analysis of variance.

Alexa Fluor 568 anti-rabbit IgG secondary antibody was from Molecular Probes (Eugene, OR). SuperSignal substrate for chemiluminescence detection, Immunopure IgG elution buffer, biotin-HPDP, and horseradish peroxidase conjugated to secondary antibodies and to avidin (avidin-HRP) were from Pierce. PCR primers were synthesized by Integrated DNA Technologies (Coralville, IA). Streptavidin-agarose, protein-A-agarose, and all of the other reagents were from Sigma.

Cell Culture and Drug Treatment—BAEC were obtained from Cambrex (Walkersville, MD) and maintained in culture on gelatin-coated 100-mm culture dishes with Dulbecco's modified Eagle's medium supplemented with fetal bovine serum (10% v/v) and penicillin-streptomycin (2%). Experiments were performed with cells between passages 5 and 8. Cultures were serum-starved overnight before experiments and drug treatments were performed as described (13). COS-7 cells were obtained from ATCC (Manassas, VA) and maintained on uncoated culture dishes in the same medium as BAEC (14).

Plasmid Construction and Transfection—The plasmid pKENH encoding HA epitope-tagged wild-type bovine eNOS cDNA (GenBank™ accession number M89952 (46)), its parent plasmid pBKCMV (Stratagene), and eNOS cDNA constructs containing mutations at Ser^{116} and Ser^{1179} have been described previously (15–17). Plasmids encoding eNOS mutants deficient in myristoylation ($eNOS^{myr-}$) and palmitoylation ($eNOS^{palm-}$) have been previously characterized in detail (12, 18, 19). pKENH served as the template for creation of eNOS constructs where Cys^{96} and/or Cys^{101} were mutated to Ser by PCR mutagenesis using a two-step approach (20). In the first step, one fragment was generated with the forward primer for the specific mutation site (described below) plus the reverse primer that subtends the eNOS BglII site (5′-TGAGGCAGAGATCTTCACCG-3′). The second fragment was generated with the reverse mutant primer (see below) plus the forward primer subtending the EcoRI site in the polylinker of the plasmid (5′-CGCGAATTCGAAGGAGCCAC-CATGGGCAACTTGAAGAG-3′). The two fragments were then mixed, and the final product was amplified using the EcoRI and BglII primers. The primer sequences for PCR-directed mutagenesis of eNOS Cys^{96} to Ser were: forward, 5′-GGCCCAGCACTCCCAGGTGCTGCCTGGG-3′; reverse, 5′-CCCAGGCAGCACCTGGGAGTGCTGGGCC-3′. For mutagenesis of eNOS Cys^{101} to Ser, the primer sequences were: forward, 5′-GGCCCTGCACTCCCAGGTGCAGCCTGGG-3′; reverse, 5′-CCCAGGCTGCACCTGGGAGTGCAGGGCC-3′. To create the double-mutant, $eNOS^{C96S/C101S}$, $eNOS^{C96S}$ was used as the template for the primers: forward, 5′-GGCCCAGCACTCCCAGGTGCAGCCTGGG-3′; reverse, 5′-CCCAGGCTGCACCTGGGAGTGCTGGGCC-3′. After molecular cloning of the fragments back into the EcoRI/BglII-restricted parental plasmid, the nucleotide sequence was confirmed by standard dideoxynucleotide-sequencing methods (University of Maine DNA Sequencing Laboratory). BAEC and COS-7 cells were transfected with the plasmids using FuGENE 6 (Roche Applied Science) according to the manufacturer's protocol. The plasmid encoding a fusion of eNOS to the enhanced green fluorescent protein (eNOS-EGFP) has been described previously (19).

Preparation of Cellular Lysates and Immunoprecipitation—100-mm dishes of cells were washed twice with ice-cold phosphate-buffered saline and harvested by scraping cells into 1 ml of lysis buffer comprised of Tris (20 mM, pH 7.4), Nonidet P-40 (1% v/v), deoxycholate (2.5% w/v), NaCl (150 mM), Na_3VO_4 (2 mM), EDTA (1 mM), NaF (1 mM), and neocuproine (100 μM) supplemented with a mixture of protease inhibitors (17). Lysates were rocked at 4 °C for 30 min and centrifuged at 14,000 × *g* for 15 min. A 1:100 dilution of eNOS polyclonal anti-serum or 4 μg/ml anti-HA monoclonal antibody 12CA5 was incubated with 1 ml of the supernatants at 4 °C with rocking for 1–16 h. After the addition of protein-A/G-agarose and another hour of rocking at 4 °C, the beads were washed extensively with lysis buffer. eNOS was then eluted from the beads and biotinylated according to the biotin switch method essentially as described (21) or released for SDS-PAGE and immunoblot by boiling in SDS-sample buffer containing β-mercaptoethanol as described previously (19). The biotin switch-processed eNOS was then separated by low temperature non-reducing SDS-PAGE for Western blot with avidin-HRP (21) or concentrated further with streptavidin-agarose, eluted by boiling with SDS-sample buffer, and then subjected to SDS-PAGE under reducing conditions for immunoblot against eNOS as described previously (22). All of the steps before biotinylation were performed under low light conditions.

Analysis of eNOS Dimer Stability—The thermal stability profile of recombinant eNOS expressed in COS-7 cells was determined using low temperature SDS-PAGE essentially as described (23). The lysates were prepared from COS-7 cells transfected with plasmids encoding recombinant eNOS by scraping the cells into lysis buffer as described above, except that rocking of the lysates at 4 °C was done for 15 min and centrifugation was conducted for 5 min (17). The supernatants were then mixed with SDS-sample buffer and incubated for 30 min at 0, 20, 30, 40, and 50 °C before low temperature SDS-PAGE (23).

Western Blots—After separation by SDS-PAGE, proteins were electroblotted onto nitrocellulose membranes. To detect biotinylated eNOS, these nitrocellulose membranes were blocked with 5% bovine serum albumin in Tris-buffered saline containing 0.1% Tween 20 before incubation with avidin-HRP in 5% bovine serum albumin/Tris-buffered saline containing 0.1% Tween 20 according to the manufacturer's instructions. Because the gels that are used to detect biotinylated proteins are electrophoresed under non-reducing conditions, the protein bands tend to bend and blur more than with standard reducing SDS-PAGE. To detect total eNOS after blotting with avidin-HRP, membranes were stripped using the Immunopure IgG elution buffer for 24 h at room temperature. All of the immunoblots were performed as described previously (13). Stripping of immunoblots for reblotting was performed with ReBlot antibody stripping solution from Chemicon International (Temecula, CA). Densitometric analyses of autoradiographs were done using a ChemiImager 400 (Alpha Innotech, San Leandro, CA).

Subcellular Fractionation and Measurement of eNOS Activity—eNOS activity was analyzed either in lysates or subcellular fractions prepared from 100-mm dishes of transfected COS-7 cells. Subcellular fractionation was performed essentially as described with the exception that 10 μM tetrahydrobiopterin was added to the cell harvest buffer (buffer 1) comprised of Tris (50 mM, pH 7.4), EDTA (0.1 mM), EGTA (0.1 mM), and β-mercaptoethanol (2 mM) with a mixture of protease inhibitors (24). After centrifugation of lysates (2,000 × *g* for 5 min at 4 °C), resuspension in buffer 1, and 10-s sonication using a Branson 450 sonifier (Branson Ultrasonic, Danbury, CT) at 20% nominal converter amplitude, the particulate and soluble fractions were resolved by ultracentrifugation (100,000 × *g* for 30 min) and the particulate fraction was resuspended in an equal volume of buffer 1 (24). Protein concentrations were determined using the Bradford reagent (Bio-Rad), and eNOS activity was determined by measuring the conversion of L-[^{3}H]arginine to L-[^{3}H]citrulline by anion-exchange chromatography, essentially as described with the exception that the reaction mixture did not contain dithiothreitol and incubation in the reaction mixture was at 30 °C for 30 min (25). Activity assays of purified eNOS isolated from a baculovirus expression system were performed as described previously (26).

Confocal Fluorescence Microscopy—BAEC grown on coverslips were transfected with plasmids encoding eNOS-EGFP and HA-tagged $eNOS^{C96S/C101S}$ at 50–60% confluence using FuGENE 6. Cell fixing, permeabilization, incubation with polyclonal anti-HA antibody (1:250 dilution), Alexa Fluor 568 anti-rabbit IgG secondary antibody (1:850 dilution), mounting, and imaging at the Nikon Imaging Center at Harvard Medical School were performed as described previously (27). Images were processed using two-dimensional no-neighbors deconvolution by MetaMorph (Universal Imaging, Downington, PA) before three-dimensional reconstruction.

Other Methods—Mean values for individual experiments are plotted ± S.E. Data plotting and statistical analyses (ANOVA) were performed using Origin software (OriginLab, Northampton, MA). A p value <0.05 was considered statistically significant.

RESULTS

Dynamic eNOS S-Nitrosylation in Endothelial Cells—Our initial experiments explored the hypothesis that eNOS is *S*-nitrosylated in endothelial cells. We exploited a method developed to detect endogenously *S*-nitrosylated proteins in cell lysates by biotinylation. After blocking free protein sulfhydryls with methyl methanethiosulphonate, the cell lysates are treated with ascorbate to reduce *S*-nitrosothiols, which are then labeled with a biotinylated active site reagent (28). This "biotin switch" approach allows for reliable detection of protein *S*-nitrosothiols by Western blot analyses.

We found that when eNOS from resting BAEC is processed by the biotin switch method, a robust signal is detected in Western blots probed with avidin-HRP. We then performed characterizations of agonist-induced changes in eNOS *S*-nitrosylation using VEGF because of its robust eNOS agonist activity (29). We had initially anticipated that eNOS *S*-nitrosylation might increase when the enzyme was activated, but we found that when BAEC are treated with VEGF (10 ng/ml for 5 min) and that eNOS *S*-nitrosylation reproducibly disappears

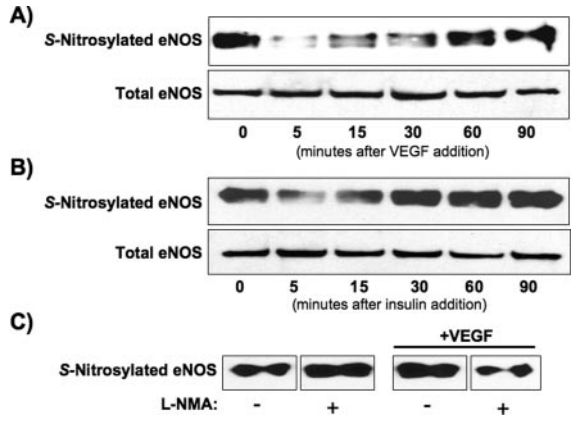

FIG. 1. **Agonist-modulated dynamic eNOS *S*-nitrosylation in BAEC.** Shown in each panel are Western blots of eNOS immunoprecipitated from cell lysates derived from BAEC and processed using the biotin switch assay. Western blot membranes were probed with avidin-HRP to detect *S*-nitrosylated eNOS as described under "Experimental Procedures." Where indicated, total eNOS was detected by reprobing stripped Western blot membranes with anti-eNOS antibody. *Panel A* shows a representative blot of three independent experiments that yielded equivalent results from BAEC treated with VEGF (10 ng/ml) for the times indicated and processed by the biotin switch method. For *B*, BAEC were treated with insulin (1 μM) for the times indicated before biotin switch analysis. For *C*, BAEC were preincubated for 60 min with L-NMA (5 mM) or vehicle and then incubated with VEGF (10 ng/ml) or its vehicle for an additional 60 min. eNOS was then harvested from the cells and processed by the biotin switch method. The blot shown is representative of three independent experiments that yielded equivalent results. Densitometric analysis of pooled data revealed that preincubation of BAEC with L-NMA before VEGF treatment reduced the extent of eNOS renitrosylation by 56 ± 0.1% ($n = 3$, $p < 0.05$) compared with control cells.

($n = 7$). As shown in Fig. 1*A*, we performed a time course of VEGF treatments to further analyze changes in eNOS *S*-nitrosylation. We found that eNOS in resting BAEC is *S*-nitrosylated and that the enzyme undergoes rapid denitrosylation after 5 min of VEGF-treatment. After this nadir of *S*-nitrosylation, eNOS is progressively renitrosylated back to basal levels over ~60 min. Treatment of BAEC with insulin, a less robust eNOS agonist (30), produces comparable results (Fig. 1*B*). We chose to focus on analyses of eNOS *S*-nitrosylation responses to VEGF, because this agonist has been characterized extensively as a potent eNOS agonist in these cells (31).

eNOS Renitrosylation Requires NO Synthase Activity—The renitrosylation of eNOS after agonist-modulated denitrosylation suggested to us that eNOS *S*-nitrosylation is dependent on eNOS activity. To test the dependence of eNOS *S*-nitrosylation on NOS activity, we pretreated BAEC with the NOS inhibitor *N*-methyl-L-arginine (L-NMA, 5 mM, 1 h) and then added VEGF (10 ng/ml) or its vehicle for 1 h before harvesting eNOS for biotin switch (32). Incubation of BAEC with L-NMA neither substantively decreases the level of basal eNOS *S*-nitrosylation nor blocks agonist-induced denitrosylation. However, as shown in Fig. 1*C*, L-NMA significantly attenuated the extent of renitrosylation of the enzyme after agonist treatment ($n = 3$, $p < 0.05$).

eNOS Phosphorylation, Subcellular Targeting, and S-Nitrosylation—In parallel with our analyses of dynamic changes in eNOS *S*-nitrosylation, BAEC were also analyzed for VEGF-modulated changes of eNOS phosphorylation at Ser^{1179}. Phosphorylation at Ser^{1179} is correlated with VEGF-modulated increases in eNOS activity and can be blocked by the phosphoinositide 3-kinase inhibitor wortmannin (29, 31). As shown in Fig. 2*A*, the time course of eNOS phosphorylation at Ser^{1179} was inversely related to the extent of eNOS *S*-nitrosylation (Fig. 1*A*).

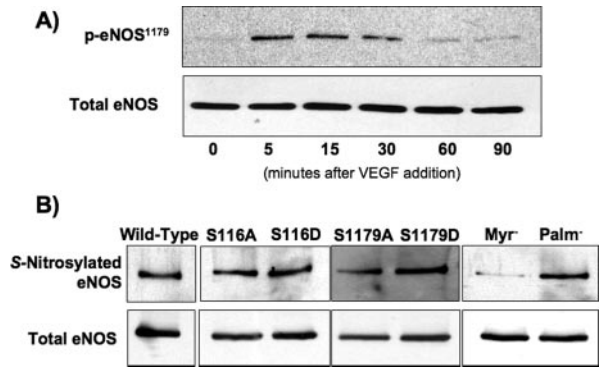

FIG. 2. **eNOS phosphorylation, *S*-nitrosylation, and subcellular targeting.** Shown in each panel are representative blots of at least three independent experiments that yielded equivalent results. *Panel A*, lysates of BAEC treated with VEGF (10 ng/ml) for the times indicated were separated by SDS-PAGE and analyzed in immunoblots probed with antibodies against phospho-eNOS^{Ser1179} or total eNOS as indicated in the legend. For *panel B*, eNOS immunoprecipitated from COS-7 cells transfected with plasmids encoding wild-type eNOS or eNOS constructs mutated at phosphorylation or acylation sites (as indicated) was processed by the biotin switch method, captured with streptavidin-agarose, and released by boiling in SDS-sample buffer. *S*-Nitrosylated eNOS (*upper blots*) and total eNOS levels in cell lysates (*lower blots*) were detected by probing immunoblots with anti-eNOS antibody, as described under "Experimental Procedures."

Because agonist-induced changes in the pattern of eNOS phosphorylation are influenced by eNOS subcellular localization (19), we decided to explore the relations among eNOS phosphorylation, subcellular targeting, and *S*-nitrosylation. We first explored whether mutation of important eNOS phosphoresidues to "phosphonull" Ala or "phosphomimetic" Asp had any effect on eNOS *S*-nitrosylation. After immunoprecipitation of the eNOS mutants from lysates prepared from transfected COS-7 cells, eNOS was biotinylated by the biotin switch method, concentrated using streptavidin-agarose, and eluted by boiling in SDS-sample buffer (22). *S*-Nitrosylated eNOS was then detected in immunoblots probed with eNOS antibodies. As shown in Fig. 2*B*, biotin switch analyses of eNOS mutants at Ser^{116} and Ser^{1179} (sites of agonist-modulated dephosphorylation and phosphorylation, respectively) revealed no substantive differences in *S*-nitrosylation compared with wild-type eNOS (Fig. 2*B*) (16, 29, 31).

We also explored the influence of eNOS targeting on enzyme *S*-nitrosylation by transfecting COS-7 cells with cDNA encoding wild-type eNOS, which is membrane-associated, with an acylation-deficient eNOS mutant (eNOS^{myr-}) that is targeted exclusively to the cytosol or with a palmitoylation-deficient eNOS (eNOS^{palm-}) that has an intermediate phenotype (19). As shown in Fig. 2*B*, when eNOS^{myr-} is immunoprecipitated from transfected COS-7 cell lysates and processed by the biotin switch method, almost no *S*-nitrosylation signal is detected, in contrast to the robust signal of wild-type eNOS (91 ± 0.1% decrease in *S*-nitrosylation for the eNOS^{myr-} mutant relative to wild-type eNOS, $n = 3$, $p < 0.001$). The palmitoylation-deficient eNOS (eNOS^{palm-}) mutant showed levels of *S*-nitrosylation that were not substantively different from the wild-type eNOS in transfected COS-7 cells (Fig. 2*B*). There is no substantive difference between the NO synthase activity levels of wild-type eNOS and eNOS^{myr-} in lysates prepared from transfected COS-7 cells (data not shown and Refs. 12, 33).

S-Nitrosylation Inhibits eNOS Activity—We next performed experiments using eNOS purified to homogeneity from a baculovirus expression system to explore whether *S*-nitrosylation regulates eNOS activity (26). As shown in Fig. 3, incubation of purified eNOS with 10 mM ascorbate (which reduces nitrosothiols) enhances eNOS activity to 120 ± 0.1% control sample

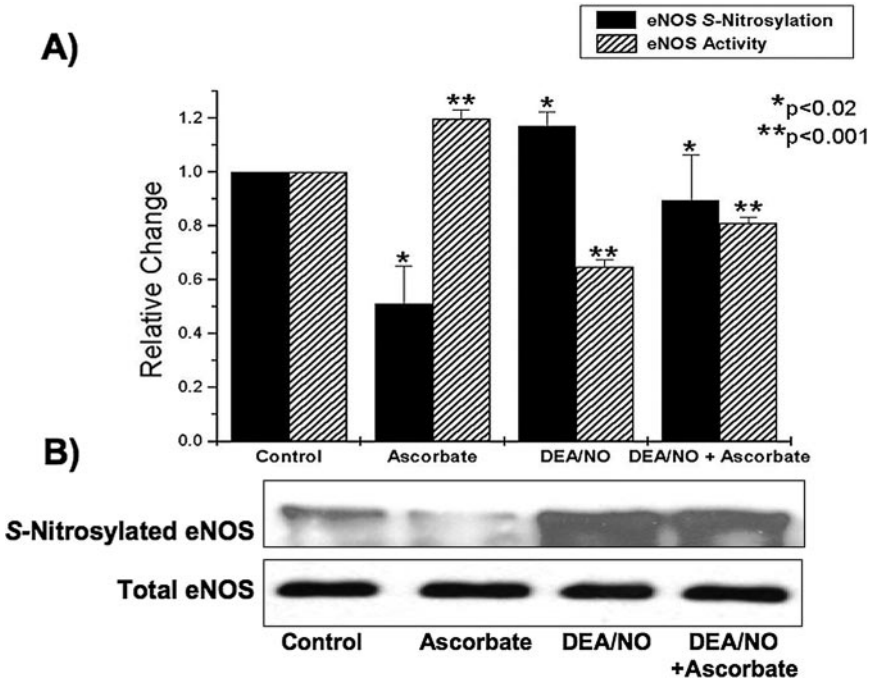

FIG. 3. **Effect of NO on *S*-nitrosylation and enzyme activity of purified eNOS.** eNOS was purified to homogeneity from insect Sf9 cells infected with recombinant baculovirus encoding wild-type eNOS, analyzed in enzyme activity assays, and processed for quantitation of *S*-nitrosylation using the biotin switch method. *Panel A* shows the results of eNOS activity assays using purified eNOS incubated under various conditions as shown: control incubation (DEA/NO aged over 48 h); ascorbate (10 mM); freshly-prepared DEA/NO (50 μM); or both ascorbate and DEA/NO. eNOS activity was assayed by measuring conversion of L-[^{3}H]arginine to L-[^{3}H]citrulline as described under "Experimental Procedures." Changes in eNOS *S*-nitrosylation were determined by densitometric analysis of pooled data from autoradiographs of samples processed by biotin switch (a representative blot is shown in *B*). Statistical analysis was performed using ANOVA; *p* values are shown in the figure. These analyses reveal that ascorbate treatment both increases eNOS activity and reduces enzyme *S*-nitrosylation, whereas DEA/NO has exactly the opposite effects. The addition of ascorbate to DEA/NO-treated eNOS results in a significant restoration of enzyme activity relative to enzyme activity with DEA/NO alone. *B*, the blot shown is representative of three independent experiments that yielded equivalent results.

activity ($n = 4, p < 0.001$) while reducing eNOS *S*-nitrosylation intensity to 51 ± 0.1% control ($n = 3, p < 0.02$). The NO donor DEA/NO (50 μM) attenuates eNOS enzyme activity to 65 ± 0.1% control levels ($n = 4$, $p < 0.001$), whereas eNOS *S*-nitrosylation levels increased to 117 ± 0.1% control sample intensity ($n = 3, p < 0.02$). The addition of ascorbate (10 mM) to the reaction containing *S*-nitrosylated eNOS significantly relieved the enzyme inhibition induced by DEA/NO, returning it to 81 ± 0.1% of the control (eNOS plus aged DEA/NO) activity level ($n = 4, p < 0.001$) and reducing *S*-nitrosylation levels to 89 ± 0.2% of the control ($n = 3, p < 0.02$).

Identification of eNOS S-Nitrosylated Cysteines—In our next series of experiments, we sought to identify the specific sites of eNOS *S*-nitrosylation. The zinc-tetrathiolate motif present in eNOS has been proposed as an *S*-nitrosylation target (4), and a recent report (34) has confirmed this possibility, showing that eNOS releases Zn^{2+} and is inactivated by treatment with exogenous NO donors *in vitro*. We hypothesized that the cysteines comprising eNOS zinc-tetrathiolate complex (Cys^{96} and Cys^{101} of each subunit) are the targets of endogenous *S*-nitrosylation and used PCR-directed mutagenesis to construct site-specific mutants of eNOS, changing the cysteines individually and collectively to serine.

We used the biotin switch method to test for *S*-nitrosylation of eNOS mutants at Cys^{96} and/or Cys^{101}. As shown in Fig. 4*A*, only the wild-type recombinant eNOS is *S*-nitrosylated when expressed in COS-7 cells. Neither the single nor double eNOS mutants at Cys^{96} and/or Cys^{101} undergo *S*-nitrosylation despite robust protein expression of all of the constructs. We also determined the phosphorylation patterns of the different eNOS constructs by immunoblot analyses using phosphorylation state-specific antibodies raised against different eNOS phosphopeptides. As shown in Fig. 4*B*, phosphorylation of wild-type eNOS and the eNOS constructs mutated at Cys^{96} and/or Cys^{101} was equivalent at Ser^{116}, Thr^{497}, and Ser^{1179} residues in transfected COS-7 cells.

We next explored the agonist-responsiveness of the nitrosylation-deficient $eNOS^{C96S/C101S}$ mutant by testing the effects of VEGF on Ser^{1179} phosphorylation in BAEC transfected with the wild-type eNOS and $eNOS^{C96S/C101S}$. For these experiments in BAEC, we immunoprecipitated the recombinant constructs using antibodies directed against the HA epitope tag (18, 19). As shown in Fig. 4*C*, basal phosphorylation at Ser^{1179} is the same for wild-type eNOS and $eNOS^{C96S/C101S}$. Furthermore, both wild-type eNOS and the *S*-nitrosylation-deficient $eNOS^{C96S/C101S}$ mutant undergo robust VEGF-induced phosphorylation at Ser^{1179}. For both the wild-type eNOS and $eNOS^{C96S/C101S}$ enzymes, phosphorylation at Ser^{1179} is completely blocked by 30-min preincubation of BAEC with the phosphoinositide 3-kinase inhibitor wortmannin (data not shown). The level of the VEGF-induced increase in Ser^{1179} phosphorylation is 42 ± 0.1% lower in the $eNOS^{C96S/C101S}$ mutant compared with the wild-type enzyme ($n = 4, p < 0.01$). A decreased level of VEGF-modulated Ser^{1179} phosphorylation of $eNOS^{C96S/C101S}$ relative to the wild-type enzyme was seen throughout a 60-min time course following the addition of VEGF (data not shown).

To establish that the failure to document *S*-nitrosylation of the $eNOS^{C96S/C101S}$ mutant eNOS is not simply due to a loss of enzyme activity, we performed NO synthase activity assays in lysates of COS-7 cells transfected with wild-type eNOS and the *S*-nitrosylation-deficient $eNOS^{C96S/C101S}$ mutant. The mean eNOS activity from COS-7 cells transfected with wild-type eNOS was 39 ± 17 pmol of L-[^{3}H]citrulline/min/mg protein, and

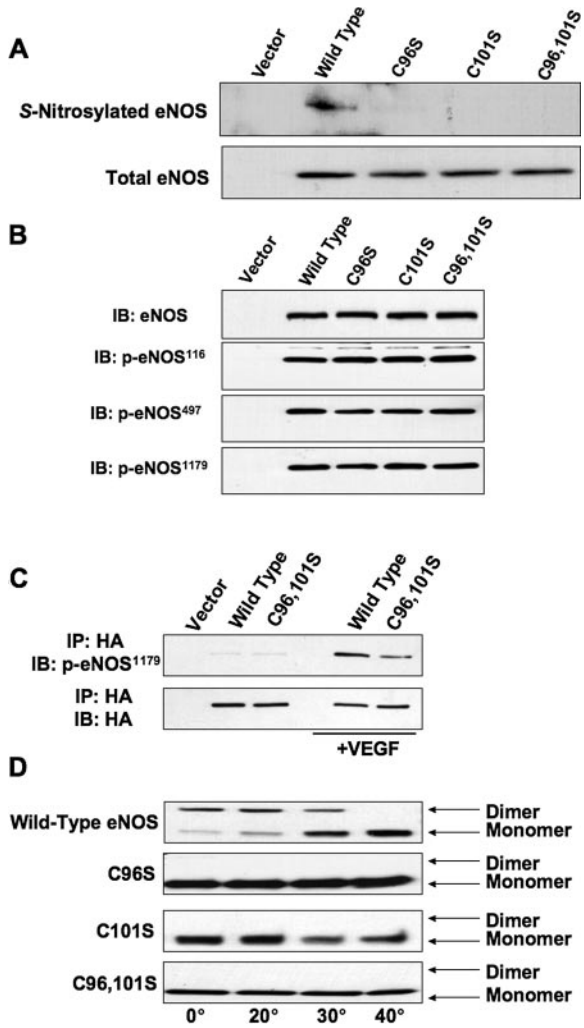

FIG. 4. **Characterization of *S*-nitrosylation, phosphorylation and dimer stability of wild-type eNOS and eNOS mutants at Cys[96] and/or Cys[101].** Shown in each panel are representative Western blots from at least three independent experiments that yielded equivalent results. For *panel A*, COS-7 cells were transfected with plasmids encoding wild-type eNOS or eNOS constructs mutated at Cys[96] and/or Cys[101]. eNOS was immunoprecipitated from lysates of transfected cells and processed according to the biotin switch method. Biotinylated eNOS was then captured with streptavidin-agarose and released by boiling in SDS-sample buffer. Immunoblots were probed with anti-eNOS antibody to detect *S*-nitrosylated eNOS (*upper blot*) or total eNOS levels in cell lysates (*lower blot*), as described under "Experimental Procedures." For *B*, COS-7 cells were transfected with plasmids encoding eNOS constructs as indicated. eNOS phosphorylation patterns were determined by probing Western blots with phosphospecific antibodies as described under "Experimental Procedures." *IB*, immunoblotting. For *C*, BAEC were transfected with plasmids encoding the wild-type eNOS and eNOS$^{C96S/C101S}$ constructs. 48 h after transfection, cells were serum-starved overnight before the addition VEGF (10 ng/ml, 5 min). Cells were lysed, and the eNOS constructs immunoprecipitated (*IP*) with antibodies against the HA epitope as described under "Experimental Procedures." After separation by SDS-PAGE, the immunoprecipitated eNOS was probed with antibodies against phospho-eNOS^{Ser1179} or the HA epitope as indicated. Preincubation with wortmannin (500 nM, 30 min) completely blocks VEGF-induced phosphorylation of each eNOS construct (data not shown). Densitometric analysis of pooled data shows that the VEGF-modulated increase in Ser^{1179} phosphorylation is 42 ± 0.1% less for the eNOS$^{C96S/C101S}$ mutant ($n = 4$, $p < 0.01$ by ANOVA). For *D*, eNOS dimer stability assays were performed in lysates prepared from COS-7 cells that had been transfected with plasmids encoding wild-type eNOS and the mutant eNOS constructs as indicated. Following incubation for 30 min at the temperatures indicated, eNOS dimers and monomers were resolved by low temperature SDS-PAGE and were visualized in immunoblots probed with anti-eNOS antibody, as described under "Experimental Procedures." Assays performed under reducing or non-reducing conditions yielded similar outcomes.

the eNOS$^{C96S/C101S}$ mutant attained only 50 ± 0.1% of the activity level of the wild-type enzyme ($n = 3$, $p < 0.01$) in lysates prepared from these transfected cells. Moreover, we found that the activity of various *S*-nitrosylation-deficient mutant eNOS constructs was lost upon detergent solubilization of the protein. Attempts to stabilize the particulate enzyme, using a wide range of detergents, all led to a rapid loss in activity for the eNOS$^{C96S/C101S}$, hampering further attempts to purify and characterize enzymological features of the mutant enzyme. These findings are consistent with other reports that attempted to explore activity of mutant eNOS containing altered eNOS zinc-tetrathiolate cysteines (34). It is plausible that dimerization of eNOS (which is required for enzyme activity) is perturbed following mutagenesis of the Cys[96] or Cys[101] residues, which coordinate the Zn^{2+} at the eNOS dimer interface (4). To determine the stability of eNOS dimers of the mutant constructs, we performed low temperature SDS-PAGE of lysates prepared from transfected COS-7 cells (23). As shown in Fig. 4*D*, wild-type eNOS can be recovered as a dimer on low temperature SDS-PAGE and is converted into monomeric protein following heating. By contrast, no eNOS constructs with mutations of Cys[96] and/or Cys[101] can be recovered as dimeric protein in detergent-solubilized lysates of transfected COS-7 cells (Fig. 4*D*). Importantly, the wild-type enzyme is recovered as a dimer (Fig. 4*D*) while being robustly *S*-nitrosylated (Fig. 2*B*). This finding argues against *S*-nitrosylation promoting dissociation of the eNOS dimer in intact cells, even if the oligomeric structure of the eNOS cysteine-serine mutants appears to be less stable upon detergent solubilization of cellular lysates (Fig. 4*D*).

Subcellular Targeting of eNOS$^{C96S/C101S}$—We next examined the subcellular distribution of the eNOS$^{C96S/C101S}$ mutant (19). Subcellular fractionation of lysates prepared from COS-7 cells transfected with wild-type eNOS or eNOS$^{C96S/C101S}$ revealed that the NO synthase activity of both wild-type eNOS and eNOS$^{C96S/C101S}$ is recovered primarily in the particulate fraction (data not shown), in agreement with previous reports on subcellular distribution of wild-type eNOS (12). We performed cellular imaging studies in BAEC transfected with the HA epitope-tagged eNOS$^{C96S/C101S}$ mutant plus EGFP-tagged wild-type eNOS (eNOS-EGFP). eNOS-EGFP does not contain the HA epitope, so the pattern of subcellular distribution of both constructs can be imaged in the same cells. Confocal microscopy of fixed transfected cells reveals that the subcellular distribution of wild-type eNOS and eNOS$^{C96S/C101S}$ are equivalent in resting cells (Fig. 5, *A–C*). When VEGF is added (10 ng/ml, 5 min), both wild-type eNOS-EGFP and eNOS$^{C96S/C101S}$ undergo agonist-modulated translocation away from the plasma membrane (Fig. 5, *D–F*).

DISCUSSION

This report shows that eNOS undergoes *S*-nitrosylation in endothelial cells and that this process is dynamically regulated by eNOS agonists in intact cells. These studies represent the first documentation of receptor-modulated reversible *S*-nitrosylation of a signaling protein. As shown in Fig. 1, eNOS is constitutively *S*-nitrosylated in resting endothelial cells. After the addition of the eNOS agonist VEGF to BAEC, eNOS is denitrosylated and then progressively renitrosylated, resuming its original level of *S*-nitrosylation over a period of 1 h. The temporal pattern of eNOS *S*-nitrosylation may provide an important clue to the role of *S*-nitrosylation in the modulation of enzyme activity. By definition, eNOS is at its basal (lowest) level of activity in resting endothelial cells when enzyme *S*-nitrosylation is at its highest level. Following the addition of VEGF, eNOS is rapidly activated in a process associated with both an increase in enzyme phosphorylation at Ser[1179] (Fig. 2*A*)

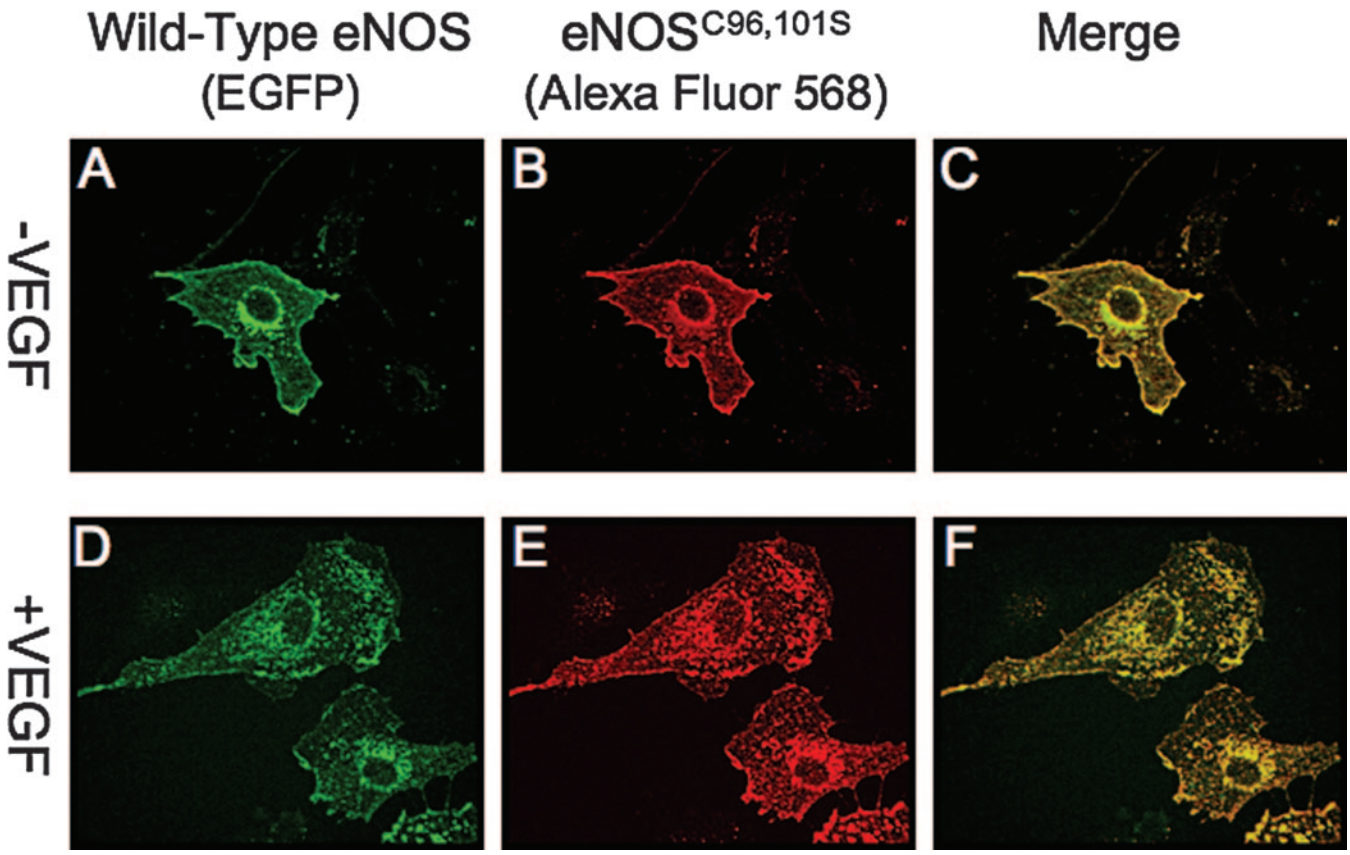

FIG. 5. **Confocal imaging of wild-type eNOS-EGFP and HA epitope-tagged eNOS$^{C96S/C101S}$ in transfected BAEC.** BAEC were transfected with plasmids encoding wild-type eNOS-EGFP and HA epitope-tagged eNOS$^{C96S/C101S}$. 48 h after transfection, BAEC were serum-starved overnight and treated with VEGF (10 ng/ml, 5 min) or its vehicle. Cells were then fixed and stained with anti-HA antibody (against the HA tag of eNOS$^{C96S/C101S}$) and a secondary antibody conjugated to Alexa Fluor 568, as described under "Experimental Procedures." Images are projections of the z-stack with scaled contrast. *Panels A*, *B*, and *C* show a vehicle-treated cell imaged for eNOS-GFP (*green*), HA epitope-tagged eNOS$^{C96S/C101S}$ (*red*), and the overlay ("merge") of the two signals (*yellow*), respectively. *Panels D*, *E*, and *F* show VEGF-treated BAEC. Cells transfected only with wild-type eNOS-EGFP (which does not contain the HA epitope) and processed identically for confocal imaging did not produce any signal in the red channel (not shown).

as well as a striking decrease in eNOS *S*-nitrosylation (Fig. 1*A*). It can be seen from the VEGF time courses shown in Figs. 1*A* and 2*A* that the nadir of eNOS *S*-nitrosylation corresponds to the peak of enzyme Ser^{1179} phosphorylation when the enzyme is maximally activated (29, 31). The enzyme is subsequently renitrosylated, corresponding with the decline in eNOS Ser^{1179} phosphorylation and the return of enzyme activity to its basal state. This renitrosylation of eNOS following VEGF treatment is markedly attenuated by the addition of the NOS antagonist L-NMA (Fig. 1*C*), indicating that eNOS *S*-nitrosylation depends acutely on eNOS activity (32). The possibility that the inducible isoform of NO synthase acts as an NO donor in this system can be excluded because inducible NO synthase is not expressed in bovine aortic endothelial cells (35).

Our data also reveal a relation between eNOS subcellular localization and *S*-nitrosylation. eNOS in resting endothelial cells associated with the plasmalemmal caveolae (36). Upon agonist stimulation, eNOS translocates from the peripheral membranes to internal membrane structures (37). The correlation between eNOS activation and translocation from peripheral to internal membrane structures prompted us to explore whether changes in eNOS *S*-nitrosylation are influenced by subcellular localization of the enzyme. We found that eNOS^{myr-}, which is localized exclusively in the cellular cytosol (12), is not *S*-nitrosylated (Fig. 2*B*). This finding suggests that targeting of eNOS to cellular membranes is required for enzyme *S*-nitrosylation or that conditions in the cellular cytosol promote denitrosylation. It is also plausible that protein-protein interactions (perhaps with caveolin) and/or distinctive redox conditions in caveolae may play a role in the regulation of eNOS *S*-nitrosylation.

Our hypothesis that *S*-nitrosylation of eNOS leads to a decrease in enzyme activity is supported further by our analyses of the effects on the pharmacologic NO donor DEA/NO on eNOS activity and *S*-nitrosylation (Fig. 3). We found an inverse relationship between eNOS enzyme activity and *S*-nitrosylation, treatment of the purified enzyme with exogenous NO donors led to eNOS *S*-nitrosylation and a decrease in enzyme activity, and this NO-induced enzyme inhibition was reversed by ascorbate in parallel with denitrosylation of the enzyme. Without doubt, ascorbate and NO donors would be expected to have pleiotropic effects, even when used in studies of a purified protein. For instance, NOS cofactors and co-substrates may be modified by the effects of NO donors and/or by redox-active reagents such as DEA/NO or ascorbate. Despite these caveats, the inverse relationship between eNOS activity and eNOS *S*-nitrosylation observed in studies of the purified protein is consistent with the model implied by the temporal pattern of eNOS *S*-nitrosylation in intact endothelial cells. eNOS *S*-nitrosylation leads to enzyme inhibition, and denitrosylation promotes enzyme activation.

These studies have also identified the zinc-tetrathiolate cysteine residues as the sites in eNOS that undergo *S*-nitrosylation in intact endothelial cells. eNOS, like the other mammalian NO synthases, contains a zinc-tetrathiolate cluster at the dimer interface, a motif previously identified as a likely target

for regulation by *S*-nitrosylation (4–6, 38). Indeed, Cys^{99} of human eNOS (corresponding to Cys^{101} of the bovine eNOS) has been identified recently as *S*-nitrosylated. Modification of this residue by *S*-nitrosylation is proposed to promote enzyme monomerization (34). However, our data suggest that it is extremely unlikely that *S*-nitrosylation of eNOS in endothelial cells leads to monomerization of the enzyme. It is clear that eNOS as extracted from resting cells is robustly *S*-nitrosylated (Fig. 1) yet is almost entirely in dimer form (Fig. 4*D*) (23). It is plausible that *S*-nitrosylation alters the dimer interface to yield an enzyme that is catalytically less efficient secondary to disruption of the intersubunit electron transfer that is required for catalysis (39). Finally, because eNOS dimerization is required for activity, our observation that $eNOS^{C96S/C101S}$ (in which both Zn^{2+}-coordinating cysteines have been mutated) retains significant enzyme activity suggests that the cell is able to maintain eNOS as an enzymatically active dimer even when the zinc-tetrathiolate has been disrupted. Indeed, published reports (6, 40) have shown that mutation of a Zn^{2+}-coordinating cysteine from each monomer of NO synthase destabilizes the enzyme but does not totally eliminate dimer formation. Our data confirm that mutation of these cysteine residues leads to destabilization of the protein, to the extent that detergent solubilization of the protein leads to a complete loss of enzyme activity and disruption of the eNOS dimer (Fig. 4*D*).

Our studies have shown that the basal phosphorylation of eNOS constructs mutated at Cys^{96} and/or Cys^{101} are equivalent to that of wild-type eNOS (Fig. 4*B*). Furthermore, for both the wild-type and $eNOS^{C96S/C101S}$ mutant eNOS, VEGF treatment promotes a significant increase in phosphorylation at Ser^{1179} (Fig. 4*C*). However, the level of VEGF-induced eNOS Ser^{1179} phosphorylation is consistently lower for the $eNOS^{C96S/C101S}$ mutant compared with the wild-type enzyme (Fig. 4*C*). This finding may suggest that agonist-modulated eNOS Ser^{1179} phosphorylation by the phosphoinositide 3-kinase/Akt pathway may be facilitated by the eNOS conformation associated with *S*-nitrosylation of the zinc-tetrathiolate cysteines, *i.e.* resting conformation of the wild-type enzyme. Confocal imaging analyses of transfected BAEC treated with vehicle or VEGF show that the subcellular distribution of wild-type eNOS and $eNOS^{C96S/C101S}$ is equivalent and reveal that both the wild-type and mutant enzymes undergo subcellular translocation in response to VEGF (Fig. 5).

Taken together, these studies show that eNOS is reversibly regulated by *S*-nitrosylation of its zinc-tetrathiolate cysteines and that cellular mechanisms mediate eNOS denitrosylation upon enzyme activation. The mechanism for denitrosylation of eNOS remains unclear, but it is possible that conformational changes in the protein may serve to expose the *S*-nitrosylated cysteine residue(s) to the high concentrations of reduced thiols (*e.g.* glutathione) characteristic of the intracellular milieu. Because trans-nitrosylation is a facile reaction, the reaction with intracellular low molecular weight thiols may represent a plausible pathway for denitrosylation of eNOS (41). This hypothesis also suggests that changes in cellular redox state might influence the denitrosylation of eNOS and provide a partial explanation for the attenuation of eNOS activity by oxidative stress (42–44). For example, the antioxidant ascorbate has been proposed to enhance eNOS activity by promoting redox stabilization of eNOS cofactors (45) but this mechanism does not exclude the possibility that ascorbate also enhances eNOS activity by reducing *S*-nitrosylated cysteines as shown in Fig. 3.

eNOS activity is complexly regulated by a constellation of spatially and temporally determined post-translational modifications and protein-protein interactions (19). *S*-Nitrosylation must now be added to this list of eNOS post-translational modifications. The dynamic receptor-mediated regulation of eNOS *S*-nitrosylation provides a potentially important mechanism for the control of NO signaling pathways in the vascular wall.

Acknowledgments—We thank Drs. Ji-Eun Kim and Steven Tannenbaum (Massachusetts Institute of Technology) and Drs. Douglas A. Mitchell and Michael Marletta (University of California, Berkeley) for helpful discussions and Dr. Gordon K. Li (Brigham and Women's Hospital) for outstanding technical assistance.

REFERENCES

1. Stuart-Smith, K. (2002) *Mol. Pathol.* **55,** 360–366
2. Andrew, P. J., and Mayer, B. (1999) *Cardiovasc. Res.* **43,** 521–531
3. Loscalzo, J., and Welch, G. (1995) *Prog. Cardiovasc. Dis.* **38,** 87–104
4. Raman, C. S., Li, H., Martasek, P., Kral, V., Masters, B. S., and Poulos, T. L. (1998) *Cell* **95,** 939–950
5. Hemmens, B., Goessler, W., Schmidt, K., and Mayer, B. (2000) *J. Biol. Chem.* **275,** 35786–35791
6. Kolodziejski, P. J., Rashid, M. B., and Eissa, N. T. (2003) *Proc. Natl. Acad. Sci. U. S. A.* **100,** 14263–14268
7. Shaul, P. W. (2002) *Annu. Rev. Physiol.* **64,** 749–774
8. He, H., Venema, V. J., Gu, X., Venema, R. C., Marrero, M. B., and Caldwell, R. B. (1999) *J. Biol. Chem.* **274,** 25130–25135
9. Davis, K. L., Martin, E., Turko, I. V., and Murad, F. (2001) *Annu. Rev. Pharmacol. Toxicol.* **41,** 203–236
10. Martinez-Ruiz, A., and Lamas, S. (2004) *Cardiovasc. Res.* **62,** 43–52
11. Stamler, J. S., Lamas, S., and Fang, F. C. (2001) *Cell* **106,** 675–683
12. Busconi, L., and Michel, T. (1993) *J. Biol. Chem.* **268,** 8410–8413
13. Igarashi, J., Erwin, P. A., Dantas, A. P. V., Chen, H., and Michel, T. (2003) *Proc. Natl. Acad. Sci. U. S. A.* **100,** 10664–10669
14. Igarashi, J., and Michel, T. (2000) *J. Biol. Chem.* **275,** 32363–32370
15. Robinson, L. J., Busconi, L., and Michel, T. (1995) *J. Biol. Chem.* **270,** 995–998
16. Kou, R., Greif, D., and Michel, T. (2002) *J. Biol. Chem.* **277,** 29669–29673
17. Bernier, S. G., Haldar, S., and Michel, T. (2000) *J. Biol. Chem.* **275,** 30707–30715
18. Robinson, L. J., and Michel, T. (1995) *Proc. Natl. Acad. Sci. U. S. A.* **92,** 11776–11780
19. Gonzalez, E., Kou, R., Lin, A. J., Golan, D. E., and Michel, T. (2002) *J. Biol. Chem.* **277,** 39554–39560
20. Ausubel, F. M., Brent, R., Kingston, R. E., Moore, D. D., Seidman, J. G., Smith, J. A., and Struhl, K. (2003) *Current Protocols in Molecular Biology Online*, John Wiley & Sons, Inc., New York
21. Kim, J.-E., and Tannenbaum, S. R. (2003) *J. Biol. Chem.* **279,** 9758–9764
22. Jaffrey, S. R., and Snyder, S. H. (2001) *Sci. STKE 2001*, PL1
23. Venema, R. C., Ju, H., Zou, R., Ryan, J. W., and Venema, V. (1997) *J. Biol. Chem.* **272,** 1276–1282
24. Prabhakar, P., Cheng, V., and Michel, T. (2000) *J. Biol. Chem.* **275,** 19416–19421
25. Balligand, J. L., Kobzik, L., Han, X., Kaye, D. M., Belhassen, L., O'Hara, D. S., Kelly, R. A., Smith, T. W., and Michel, T. (1995) *J. Biol. Chem.* **270,** 14582–14586
26. Busconi, L., and Michel, T. (1995) *Mol. Pharmacol.* **47,** 655–659
27. Gonzalez, E., Nagiel, A., Lin, A. J., Golan, D. E., and Michel, T. (2004) *J. Biol. Chem.* **279,** 40659–40669
28. Jaffrey, S. R., Erdjument-Bromage, H., Ferris, C. D., Tempst, P., and Snyder, S. H. (2001) *Nat. Cell Biol.* **3,** 193–197
29. Fulton, D., Gratton, J. P., McCabe, T. J., Fontana, J., Fujio, Y., Walsh, K., Franke, T. F., Papapetropoulos, A., and Sessa, W. C. (1999) *Nature* **399,** 597–601
30. Takahashi, S., and Mendelsohn, M. E. (2003) *J. Biol. Chem.* **278,** 30821–30827
31. Dimmeler, S., Fleming, I., Fisslthaler, B., Hermann, C., Busse, R., and Zeiher, A. M. (1999) *Nature* **399,** 601–605
32. Griffith, O. W., and Kilbourn, R. G. (1996) *Methods Enzymol.* **268,** 375–392
33. Lin, S., Fagan, K. A., Li, K. X., Shaul, P. W., Cooper, D. M., and Rodman, D. M. (2000) *J. Biol. Chem.* **275,** 17979–17985
34. Ravi, K., Brennan, L. A., Levic, S., Ross, P. A., and Black, S. M. (2004) *Proc. Natl. Acad. Sci. U. S. A.* **101,** 2619–2624
35. Nishida, K., Harrison, D. G., Navas, J. P., Fisher, A. A., Dockery, S. P., Uematsu, M., Nerem, R. M., Alexander, R. W., and Murphy, T. J. (1992) *J. Clin. Investig.* **90,** 2092–2096
36. Feron, O., Saldana, F., Michel, J. B., and Michel, T. (1998) *J. Biol. Chem.* **273,** 3125–3128
37. Prabhakar, P., Thatte, H. S., Goetz, R. M., Cho, M. R., Golan, D. E., and Michel, T. (1998) *J. Biol. Chem.* **273,** 27383–27388
38. Wink, D. A., Grisham, M. B., Mitchell, J. B., and Ford, P. C. (1996) *Methods Enzymol.* **268,** 12–31
39. Xie, Q. W., Leung, M., Fuortes, M., Sassa, S., and Nathan, C. (1996) *Proc. Natl. Acad. Sci. U. S. A.* **93,** 4891–4896
40. Chen, P. F., Tsai, A. L., and Wu, K. K. (1995) *Biochem. Biophys. Res. Commun.* **215,** 1119–1129
41. Hogg, N. (1999) *Anal. Biochem.* **272,** 257–262
42. Ting, H. H., Timimi, F. K., Boles, K. S., Creager, S. J., Ganz, P., and Creager, M. A. (1996) *J. Clin. Investig.* **97,** 22–28
43. Heller, R., Munscher-Paulig, F., Grabner, R., and Till, U. (1999) *J. Biol. Chem.* **274,** 8254–8260
44. Huang, A., Xiao, H., Samii, J. M., Vita, J. A., and Keaney, J. F., Jr. (2001) *Am. J. Physiol.* **281,** C719–C725
45. Heller, R., Unbehaun, A., Schellenberg, B., Mayer, B., Werner-Felmayer, G., and Werner, E. R. (2001) *J. Biol. Chem.* **276,** 40–47
46. Lamas, S., Marsden, P. A., Li, G. K., Tempst, P., and Michel, T. (1992) *Proc. Natl. Acad. Sci. U. S. A.* **89,** 6348–6352